**CERN-ACC-NOTE-2015-0036**

2015.09.15
Roderik.Bruce@cern.ch
Regina.Kwee@rhul.ac.uk

# Collimation with tighter TCTs at $\beta^*$=40 cm

R. Bruce, P.D. Hermes, A. Mereghetti, D. Mirarchi, E. Quaranta, S. Redaelli, B. Salvachua, G. Valentino, A. Valloni, CERN, Geneva, Switzerland
H. Garcia, R. Kwee-Hinzmann, Royal Holloway University of London, Egham, Surrey, UK

Keywords: LHC, collimation

Summary

MD 310 was carried out on August 28 2015, in order to investigate the collimation performance using nominal optics with $\beta^*$=40 cm, 2 $\sigma$ retraction collimator settings in IR7, and the very tight TCT settings which are necessary to protect the small normalized aperture. With these tight settings, we expect higher losses on the TCTs which should cause also higher beam-halo background at the experiments. During the MD, a total of 70 betatron loss maps were performed over a range of TCT settings and for different settings of the TCLAs in IR7. ATLAS and CMS were exceptionally taking data outside stable beams, in order to monitor the background. Furthermore, betatron loss maps were performed with a small momentum offset of the whole beam, induced by a shift of the RF frequency. The MD results can therefore also be used to assess the cleaning efficiency in IR7 with the $\beta^*$=40 cm optics, as well as the effects of energy offsets on the cleaning. At the end of the MD, an asynchronous dump test was performed, in order to monitor the losses on sensitive equipment with $\beta^*$=40 cm and the proposed collimator settings. This MD is one in a series meant to address various open points for the reach in $\beta^*$ in Run II.

## 1 Introduction

In order to push down $\beta^*$ to values well below the nominal 55 cm, e.g. to 40 cm, it is necessary to significantly reduce the margins in the collimation hierarchy [1, 2] in order to protect the much smaller normalized aperture in the inner triplet. The TCTs must then be moved in to a setting close to the one of dump protection in IR6, which is possible only if the optics is such that the fractional betatron phase advance from the dump kickers to the TCTs is so far away from 90° and 270° that they do not risk to receive high-intensity impacts during a beam abort failure.

Under this assumption, other constraints than the TCT robustness could limit the achiev-

able TCT setting. In particular, as the TCTs move closer to the beam, they are expected to intercept larger halo losses. This is expected to increase the beam-halo background in the experiments, as the amount of secondary shower particles escaping the TCTs and propagating to the detector scales linearly with the number of impacts on the TCT. Furthermore, the closer the TCTs get to the IR7 secondary collimators, the higher is the risk of a hierarchy breakage. Moreover, at $\beta^*$=40 cm, the chromatic $\beta$-beating is worse than at higher $\beta^*$, which could potentially cause hierarchy violations for the primary halo. Furthermore, it could influence the cleaning performance of the collimation system, when particles with large energy offsets are scattered out of the IR7 collimators.

Therefore, this MD aimed at investigating at the same time the losses on the TCTs for standard cleaning and fast failures, the resulting experimental background, and the general cleaning performance at $\beta^*$=40 cm. To do this, a large set of betatron loss maps was performed over a range of TCT settings, while a 2 $\sigma$ retraction was kept between the IR7 TCPs and TCSGs. ATLAS and CMS were exceptionally taking data outside stable beams in order to monitor the background. This MD therefore provides, together with the qualification loss maps performed at $\beta^*$=80 cm in July 2015, the only measurement so far with clean conditions for observing halo-induced background, where other sources of signals at the experiments such as luminosity or beam-gas background should be negligible in comparison. The results this MD can be used to determine a range of possible TCT settings, which is acceptable in terms of cleaning and background.

In addition, loss maps were performed for two different settings of the IR7 TCLAs, as well as for small energy errors, introduced by a change in RF frequency. At the end, an asynchronous dump test was performed.

# 2 Measurement procedure

The machine was filled with 15 pilots and 1 nominal bunch per ring. The filling scheme, which is illustrated in Fig. 1, had been conceived not to have any collisions or parasitic encounters in any IP. The energy was ramped and, at flat top, the TCTs were symmetrized with respect to the flat orbit, taking as extreme settings those used for the standard $\beta^*$=80 cm configuration. Then all crossing and separation bumps were flattened, followed by a first squeeze to $\beta^*$=80 cm and then a second step to $\beta^*$=40 cm, where the optics had previously been corrected [3]. The nominal optics was used all along the MD. The orbit was kept flat during the MD for machine protection reasons, as this was the first time ever that a nominal bunch was brought to $\beta^*$=40 cm.

Once at $\beta^*$=40 cm, the TCTs in IR1 and IR5 were aligned using the BPM buttons and positioned at 7.8 $\sigma$ (we assume always a normalized emittance of 3.5 $\mu$m throughout this note) around the closed orbit. Furthermore, the TCSGs in IR7 were moved in to 7.5 $\sigma$ to achieve a 2 $\sigma$ retraction from the TCPs, and the IR6 dump protection was also closed by 0.5 $\sigma$ to 8.6 $\sigma$. The used settings are summarized in Table 1. In this configuration, betatron loss maps were carried out for B1 and B2 in the horizontal and vertical planes. The loss maps were done by exciting the beams, one at a time, using a white-noise excitation of the transverse damper, and the resulting loss distribution around the ring was monitored using the BLMs. The TCTs were then opened in steps of 0.5 $\sigma$ up to 10.3 $\sigma$ and the four loss

| RFBucket | Bu Tot | bu/btch | Spc/ns | PSbchs | I level | RFBucket | Bu Tot | bu/btch | Spc/ns | PSbchs | I level |
|---|---|---|---|---|---|---|---|---|---|---|---|
| 1 | 1 | 1 | 0 | 1 | NOM | 401 | 1 | 1 | 0 | 1 | NOM |
| 3981 | 1 | 1 | 0 | 1 | INTR | 4541 | 1 | 1 | 0 | 1 | INTR |
| 5921 | 1 | 1 | 0 | 1 | INTR | 6481 | 1 | 1 | 0 | 1 | INTR |
| 7861 | 1 | 1 | 0 | 1 | INTR | 8421 | 1 | 1 | 0 | 1 | INTR |
| 9801 | 1 | 1 | 0 | 1 | INTR | 10361 | 1 | 1 | 0 | 1 | INTR |
| 11741 | 1 | 1 | 0 | 1 | INTR | 12301 | 1 | 1 | 0 | 1 | INTR |
| 13681 | 1 | 1 | 0 | 1 | INTR | 14241 | 1 | 1 | 0 | 1 | INTR |
| 15621 | 1 | 1 | 0 | 1 | INTR | 16181 | 1 | 1 | 0 | 1 | INTR |
| 17561 | 1 | 1 | 0 | 1 | INTR | 18121 | 1 | 1 | 0 | 1 | INTR |
| 19511 | 1 | 1 | 0 | 1 | INTR | 20071 | 1 | 1 | 0 | 1 | INTR |
| 21451 | 1 | 1 | 0 | 1 | INTR | 22011 | 1 | 1 | 0 | 1 | INTR |
| 23391 | 1 | 1 | 0 | 1 | INTR | 23951 | 1 | 1 | 0 | 1 | INTR |
| 25331 | 1 | 1 | 0 | 1 | INTR | 25891 | 1 | 1 | 0 | 1 | INTR |
| 27571 | 1 | 1 | 0 | 1 | INTR | 27831 | 1 | 1 | 0 | 1 | INTR |
| 29511 | 1 | 1 | 0 | 1 | INTR | 29771 | 1 | 1 | 0 | 1 | INTR |
| 30511 | 1 | 1 | 0 | 1 | INTR | 30871 | 1 | 1 | 0 | 1 | INTR |

Figure 1: The filling scheme used in the MD.

maps were repeated at each step.

The nominal bunches were added since the experiments might not have enough resolution to study in detail the background caused by losses from the pilot bunches. Therefore, stronger excitations were performed on the nominal bunches at one TCT setting (8.8 $\sigma$ according to the proposed setting in Ref. [2]) and plane per beam. These loss maps were carried out in B1V and B2H. Since ATLAS integrates the signal over luminosity blocks of 1 minute, these excitations were kept continuous over almost a minute in order to achieve a high integrated signal, in case the signal-to-noise ratio in the TCT scan with pilots would not turn out to be high enough.

Afterwards, a second TCT scan, with loss maps at each step but with fewer steps, was performed with the IR7 TCLAs closed from 14 $\sigma$ to 10 $\sigma$. Then two additional scans were carried out, in which a small energy offset of $\delta p/p = \pm 1.2 \times 10^{-4}$ was introduced on the whole beam, by shifting the RF frequency by 15 Hz in both directions. These offsets are close to 1 $\sigma$ in energy distribution of the beam and thus keep most particles well within the RF bucket. All settings in the different scans are summarized in Table 1. The results from the TCT scans are shown in Sec. 3, and some first comparisons to the expectations from simulations are discussed in Sec. 4.

A fifth scan was attempted with a larger $\delta p/p = 2.4 \times 10^{-4}$, however, only the innermost TCT setting could be probed, as strong losses were observed. Before most of the beams were gone, it was then decided to move directly to the final step, which was an asynchronous beam dump test with the TCTs in an extremely pessimistic configuration. More details about this are given in Sec. 5.

Table 1: Collimator settings, in units of $\sigma$ with a normalized emittance of 3.5 $\mu$m, used during the different TCT scans and the final asynchronous dump test. We show also the used momentum offset.

| Collimator | Scan 1 | Scan 2 | Scan 3 | Scan 4 | Scan 5 | As. dump |
|---|---|---|---|---|---|---|
| TCP IR7 | 5.5 | 5.5 | 5.5 | 5.5 | 5.5 | 5.5 |
| TCS IR7 | 7.5 | 7.5 | 7.5 | 7.5 | 7.5 | 7.5 |
| TCLA IR7 | 14.0 | 10.0 | 14.0 | 14.0 | 14.0 | 14.0 |
| TCP IR3 | 15.0 | 15.0 | 15.0 | 15.0 | 15.0 | 15.0 |
| TCS IR3 | 18.0 | 18.0 | 18.0 | 18.0 | 18.0 | 18.0 |
| TCL IR3 | 20.0 | 20.0 | 20.0 | 20.0 | 20.0 | 20.0 |
| TCT IR1,5 | $7.8 - 10.3$ | $7.8 - 9.8$ | $7.8 - 9.8$ | $7.8 - 9.8$ | 7.8 | 7.8 |
| TCSP IR6 | 8.6 | 8.6 | 8.6 | 8.6 | 8.6 | 8.6 |
| TCDQ IR6 | 8.6 | 8.6 | 8.6 | 8.6 | 8.6 | 8.6 |
| $\delta p/p$ | 0.0 | 0.0 | $-1.2 \times 10^{-4}$ | $1.2 \times 10^{-4}$ | $-2.4 \times 10^{-4}$ | 0.0 |

# 3 Measurement results from loss maps

## 3.1 IR7 cleaning performance

Examples of measured loss distributions around the ring for all scans, defined in Table 1, are shown in Fig. 2 for the case of horizontal losses in B1 with TCTs at 7.8 $\sigma$. The losses are normalized to the highest BLM signal in the ring, just downstream of the IR7 TCPs. It can be noted that the background noise level is relatively high, which was typical to all loss maps performed, despite of using the maximum ADT gain. After the MD, the maximum possible gain in the loss map application has been increased to allow for stronger losses.

The overall loss distribution is qualitatively similar in all cases, although there are some quantitative differences. As expected, the TCTs in IR1 and IR5 vary significantly between loss maps, even at the same TCT setting. This is discussed in more detail in Sec. 3.2. Furthermore, the maximum local cleaning inefficiency $\eta$, in the IR7 dispersion suppressor, is different between different scans. This is obvious from Fig. 3, which shows zooms in IR7 of the loss maps in Fig. 2. For this particular case of B1 and horizontal losses, it is clear that $\eta$ is worse in scans 3 and 5, where a negative energy offset was applied. As usual for measured losses, $\eta$ is calculated as the ratio between the highest cold BLM and the highest BLM in the ring (close to the primary collimators) after noise subtraction.

It is expected that $\eta$ is independent of the TCT setting, as it is dominated by the particles hitting the upstream IR7 TCP on the same turn. This assumption can be checked in Fig. 4, which shows the measured $\eta$ in both beams and planes as a function of the TCT setting in scans 1–4 (scan 5 contained only one point at 7.8 $\sigma$). Some variations in $\eta$ can be seen, but in most cases they seem uncorrelated with the TCT setting. However, scan 1 shows an apparently increasing $\eta$ with larger TCT setting. This is not observed in the other scans and not well understood.

In the assumption that the TCT setting does not influence the IR7 cleaning, we show in Fig. 5 the average of $\eta$ over the TCT settings for each beam and plane and for the different

scans. It can be seen that, as expected, $\eta$ generally improves when the TCLAs in IR7 are closed (scan 2). Furthermore, the negative energy offsets in scans 3 and 5 give a worse $\eta$, especially in the horizontal plane of B1. This is consistent with the $\eta$-values from Fig. 3. The exception to this is B2, horizontal plane, where the highest $\eta$ is found in scan 1, without energy offset. With a positive energy offset (scan 4) the results are quite similar to the reference point (scan 1) except for B2H. It is not understood why B2H should be better with an energy offset. This could be investigated further in simulations.

We compare also the achieved values of $\eta$ to what is found in standard loss maps for the 2015 physics configuration ($\beta^*$=80 cm and 0.5 $\sigma$ more open TCSGs in IR7). Typical values can be found in Ref. [4]. Comparing to the loss maps at the end of the squeeze, we observe in this MD an improvement of around 20% in B2, and 40% in B1H. For B1V, similar values are observed at $\beta^*$=40 cm and $\beta^*$=80 cm. The overall improvement in the MD configuration comes likely from the smaller retraction in IR7 between TCP and TCSG.

Furthermore, we compare the found $\eta$ to the results of MD 314 on collimation hierarchy limits [5]. Several settings were tested in this MD, among others the 2 $\sigma$ retraction in IR7 with two TCLA settings. These configurations were identical in IR7 to scans 1 and 2, except that MD 314 was performed at flat top with injection optics and not at $\beta^*$=40 cm. Nevertheless, our obtained $\eta$-values at $\beta^*$=40 cm are very comparable to the other MD.

Based on the comparisons with the standard loss maps at $\beta^*$=80 cm and MD314, we conclude that there is no significant degradation of the IR7 cleaning performance at $\beta^*$=40 cm, due to e.g. the chromatic $\beta$-beating.

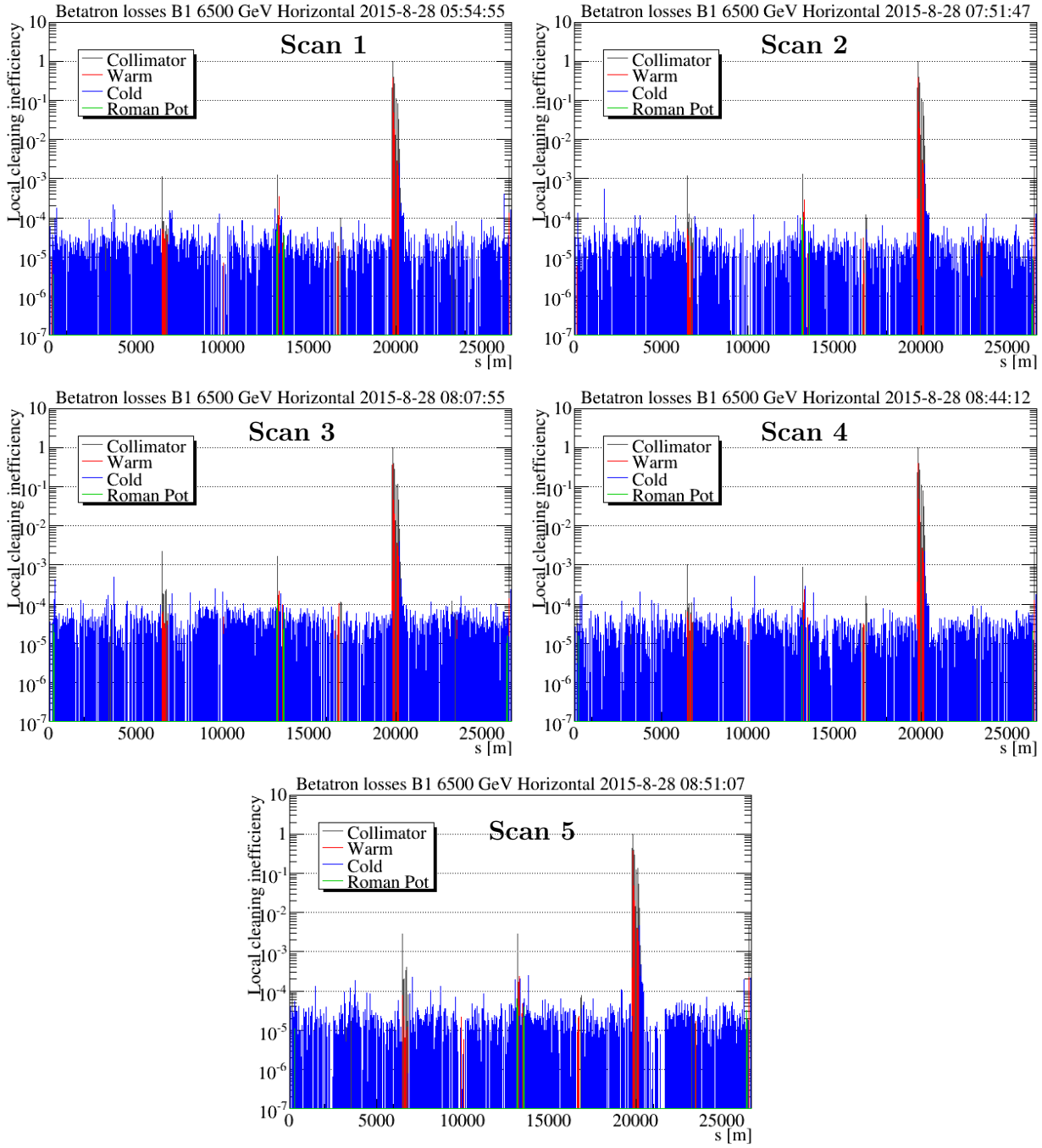


Figure 2: Noise-subtracted loss distribution around the ring following an ADT excitation in the horizontal plane of B1, with TCTs at 7.8 $\sigma$ in the different scans (see Table 1). All BLM signals have been normalized to the highest BLM in the ring, downstream of the TCPs in IR7.

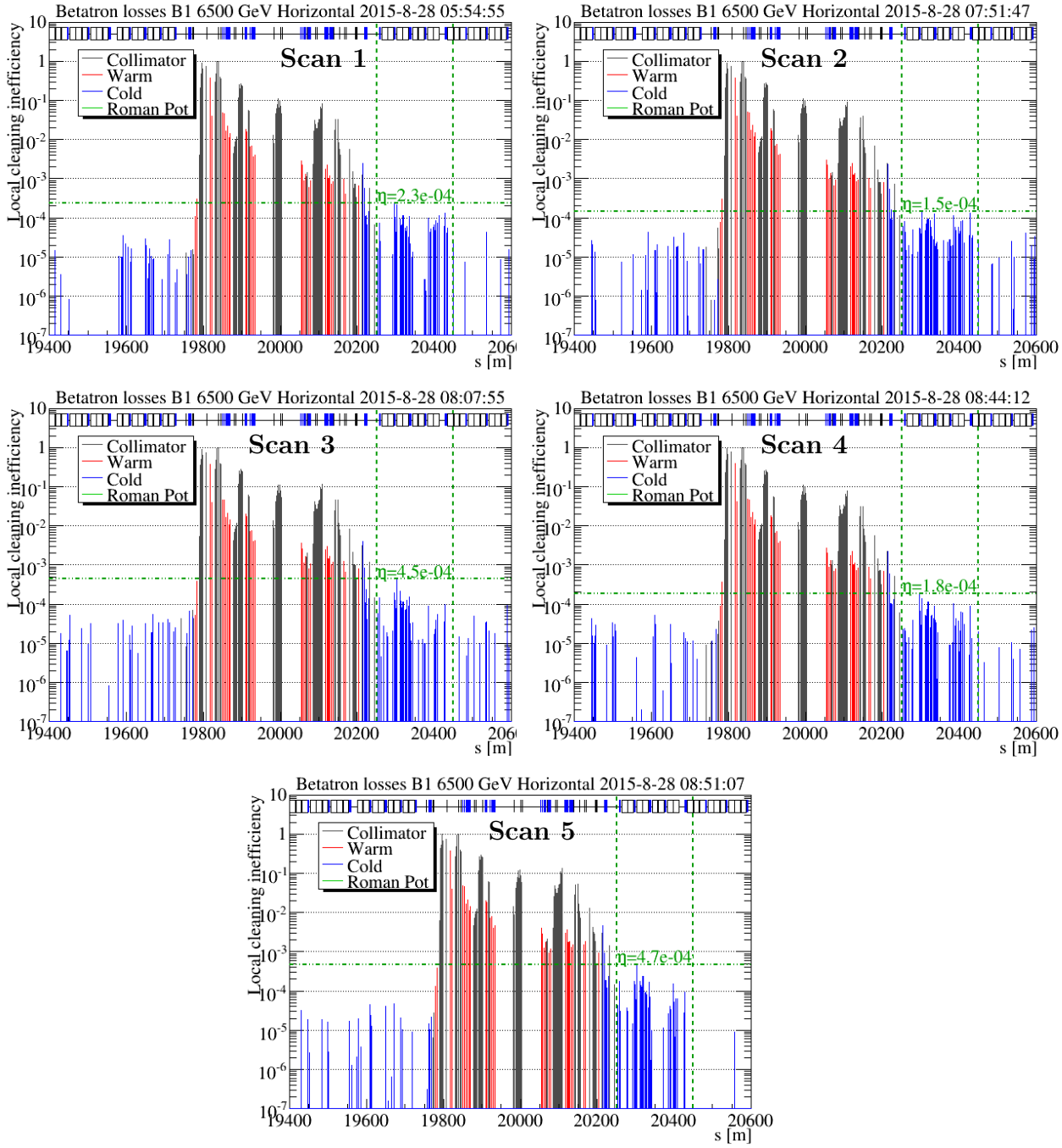


Figure 3: Noise-subtracted loss distribution in IR7 following an ADT excitation in the horizontal plane of B1, with TCTs at 7.8 $\sigma$ in the different scans (see Table 1). All BLM signals have been normalized to the highest BLM in the ring, downstream of the TCPs in IR7.

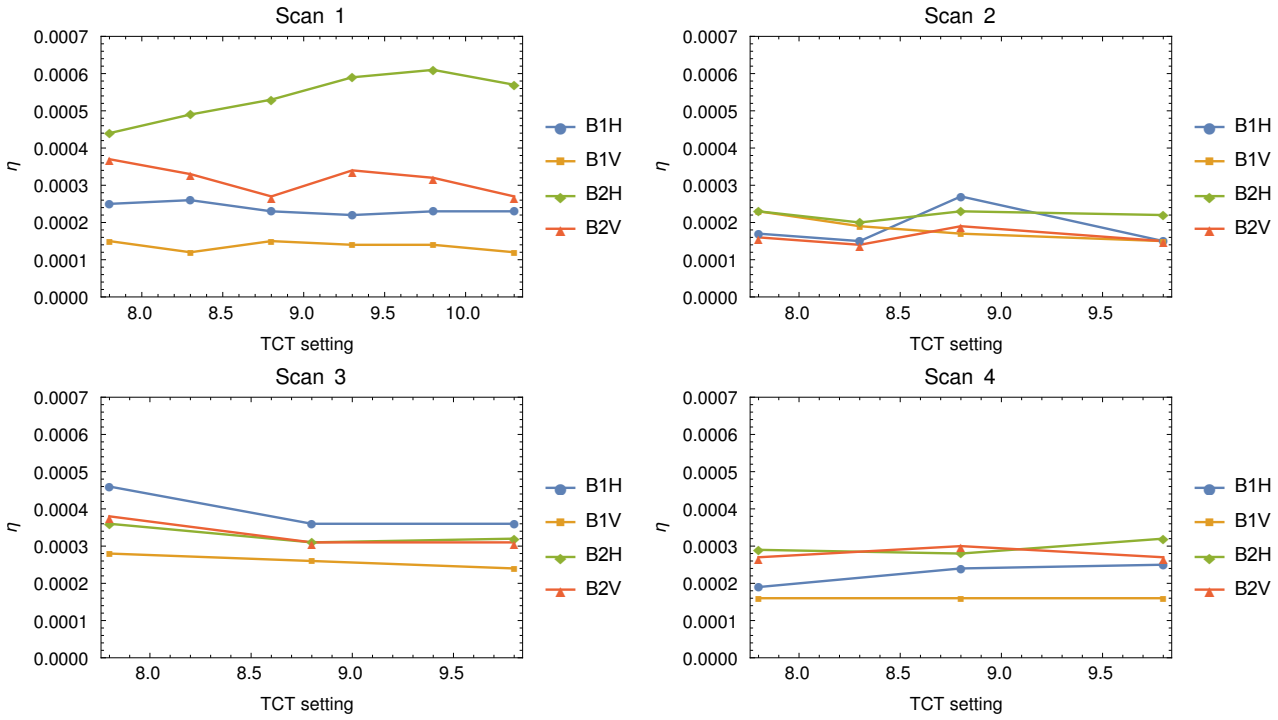


Figure 4: The maximum local cleaning inefficiency $\eta$ in the ring (measured in the dispersion suppressor of IR7). The results are shown for each TCT scan, specified in Table 1, and for each beam and plane.

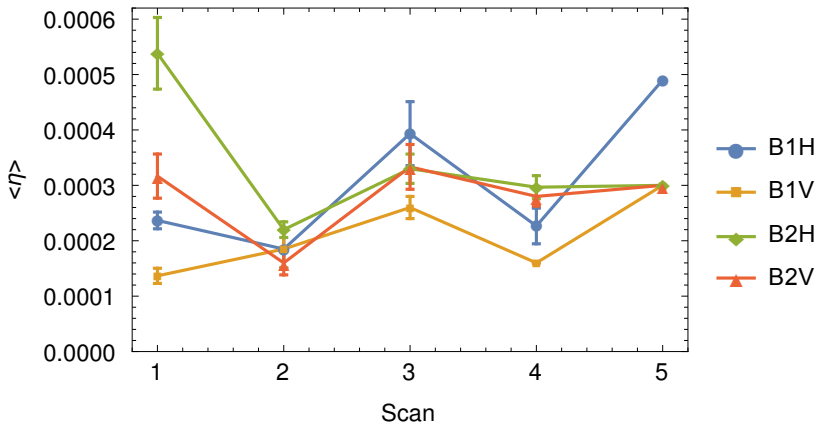


Figure 5: The maximum local cleaning inefficiency $\eta$, averaged over the different TCT settings, for each beam, plane, and TCT scan (specified in Table 1).

## 3.2 Losses on IR1 and IR5 TCTs

The analysis of losses on TCTs in IR1 and IR5 was performed using data of two groups of BLMs, those in IR1 and 5 which are directly mounted on each TCT and those that registered the highest loss in the ring at the timestamp of each loss maps for each scan. Typically, these BLMs are just downstream of the primary collimators. As for the loss maps presented above, the integration time of 1.3 seconds (running sum 9) of the BLM signal was used.

### 3.2.1 Noise substraction

The noise levels in the BLMs usually vary with time and may depend on the amount of signal seen shortly before. Therefore, it was chosen to define a time interval just before each TCT setting change of typically a minute length during which an average noise level was calculated and then substracted from the BLM signals. The time interval for noise substraction was chosen based on the clear difference between the signal and the noise of the BLMs showing the highest loss. An example is shown in Fig. 6 of the signals before (on the top) and after (on the bottom) noise substraction. This had an neglible effect on the signal in these BLMs at the time of the peak. The same time interval was used for TCT BLMs, as depicted in Fig. 7. For the TCTs, the noise subtraction is important for the more open settings where lower signal are observed.

### 3.2.2 TCT losses versus settings

The noise-substracted TCT losses were normalised to the highest BLM signal at the timestamp of the lossmap and are shown as function of the TCT setting in Fig. 8 for IR1 and in Fig. 9 for IR5. The error bars indicate the statistical fluctuations of the noise for the TCT BLM signals. In most of the cases, a clear correlation is visible: as expected, the losses are higher for tighter settings. For most of the TCT BLMs, about a factor 3 to 5 increase was found when going to tighter settings, e.g. on TCTPVs in IR1 (see Fig. 8 b,d). For a few cases, even around a factor 10 increase can be observed when reducing the TCT halfgap as in Fig. 8 (a). An exception is the BLM on TCTPV.4L5.B1 in Fig. 9 (b): here for scan 1 more than two orders of magnitude difference between the inner and outer most settings are observed, but even for the other 3 scans, the increase is about a factor 30 to 40. This is discussed more in detail in Sec. 4.

An approximately linear behaviour is seen when using a log-scale in many cases, e.g. as in Fig. 8 (a,d), but also in all figures of Fig. 9. This shows an exponential decrease of the losses versus the collimator opening, and hence also of the transverse halo population. In case the TCLAs are further closed (comparing scan 1 and scan 2) about 20% to 40% less losses are recieved, while for TCTPV.4R5.B2 (Fig. 9 (d), the losses can be reduced by up to 80 %. It should be noted also that a few outliers break the approximately exponential behaviour, e.g. a point at a TCT setting of 8.8 $\sigma$ in Fig. 9c. This remains to be understood.

Comparing the on-momentum scan 1 with the off-momentum scan 4, with a positive momentum offset, one can see that they generate very similar losses in IR1 and 5, except for the BLM attached to TCTPH.4R1. The off-momentum case with a negative frequency shift (scan 3) shows, on the other hand, significantly higher losses in several cases. For example, in B1, IR1, for TCTH and TCTV, as well as for the IR5 TCTH, the scan with the

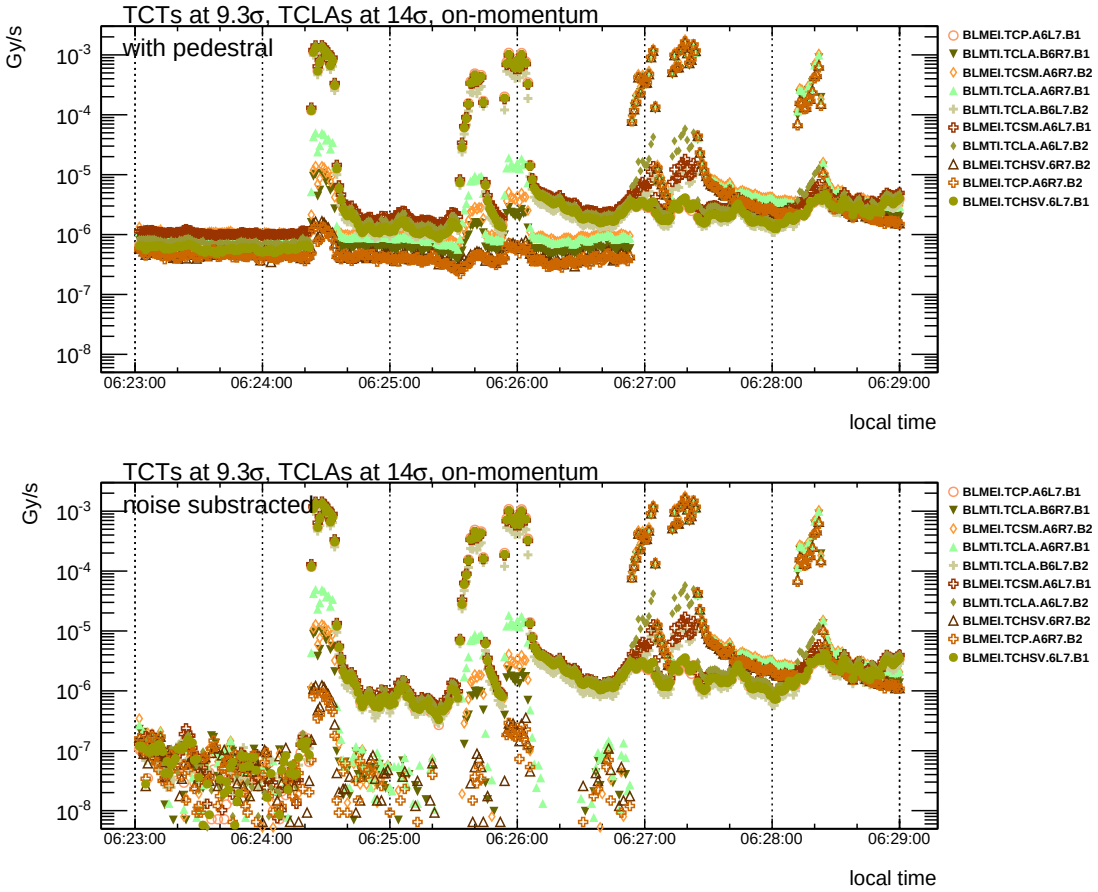


Figure 6: Example of BLM signals with highest losses before (top) and after noise substraction (bottom) when TCTs were at 9.3 $\sigma$ and TCLAs at 14 $\sigma$ (scan 1).

negative momentum offset produced higher losses than the other scans. However, the B1 TCTV in IR5 shows the opposite, with the lowest losses for the negative momentum offset. Simualtions are needed to better understand this in detail.

It should be noted that typical normalized TCT losses in the loss maps at $\beta^*$=80 cm, using the standard 2015 physics configuration, range are typically from $10^{-5}$ up to $10^{-5}$ [4]. In the loss maps from this MD with TCTs at the previously proposed setting of 8.8 $\sigma$ [2], the losses are about an order of magnitude higher as can be seen in Figs. 8 and 9. This would mean that we expect also about an order of magnitude higher backgrounds from beam halo in the $\beta^*$=40 cm configuration. Nevertheless, in Run I it was estimated that beam-gas interactions were the dominating source of machine-induced backgrounds [6], and if this is still the case in Run II, the increase of beam-halo background might not be so critical.

ATLAS and CMS were taking data during the MD, in order to verify the beam-halo background. The analysis of these data is ongoing within the experimental collaborations in order to conclude if it is acceptable for operation.

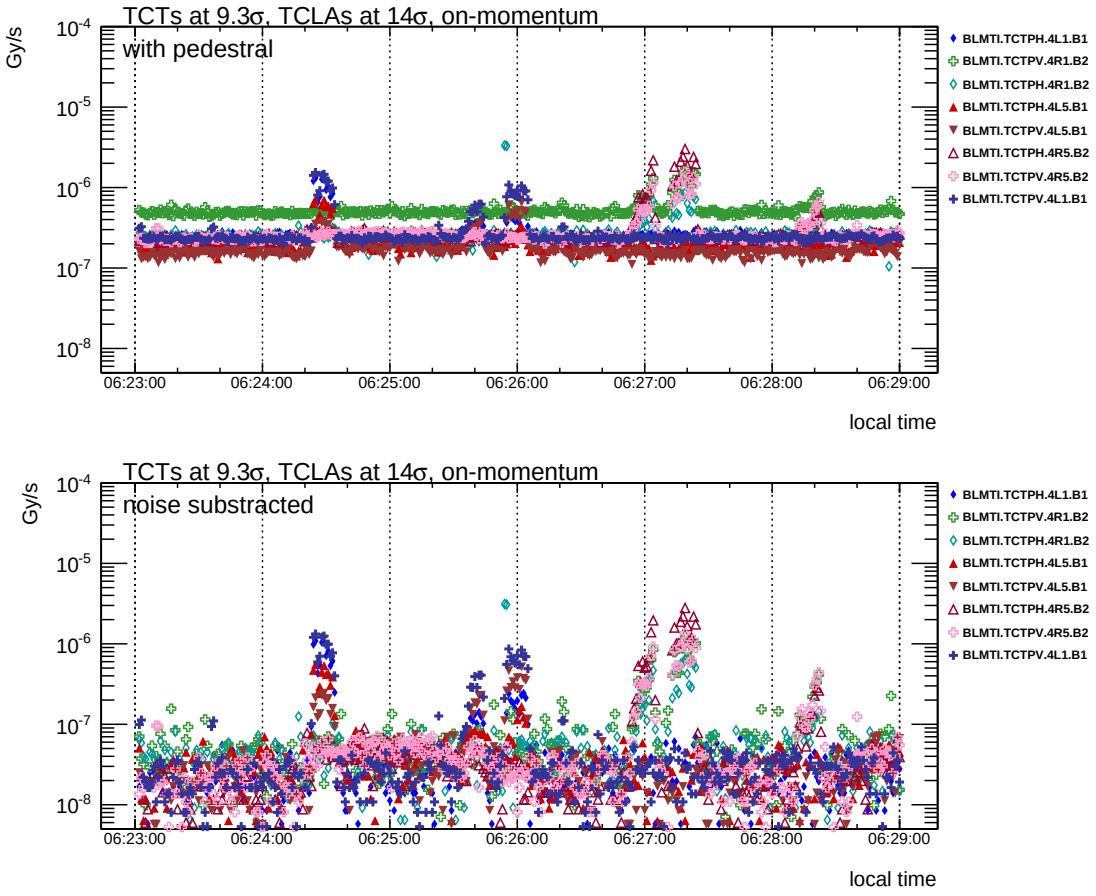


Figure 7: BLM on TCTs before (top) and after noise substraction (bottom) when set to 9.3 $\sigma$ with TCLAs at 14 $\sigma$ (scan 1).

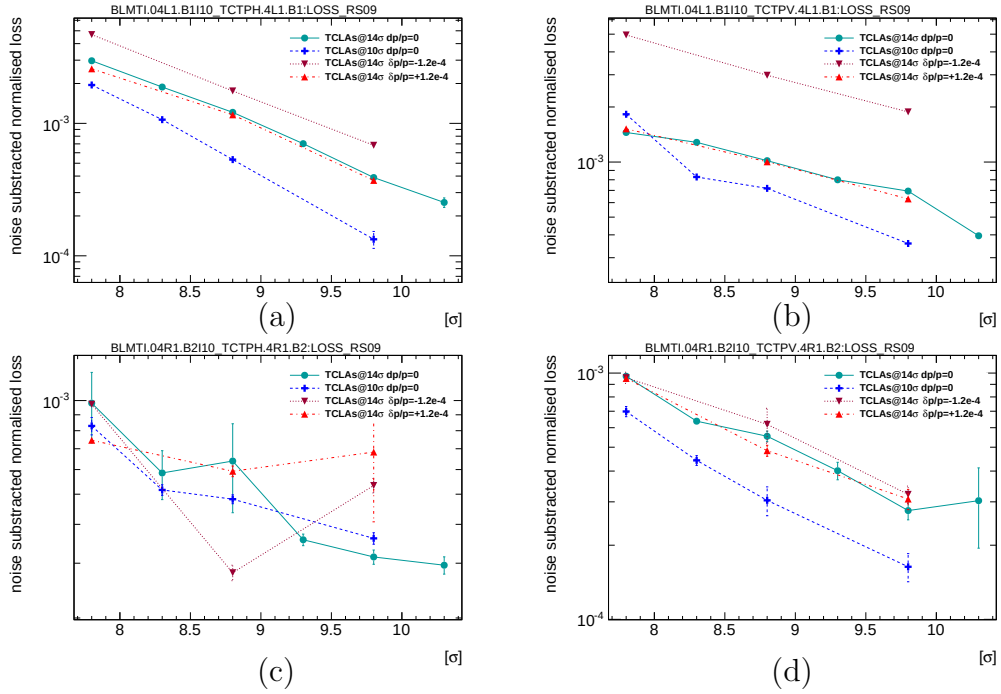


Figure 8: Losses on IR1 TCTs for B1 (a,b) and B2 (c,d) for scan 1 to 4.

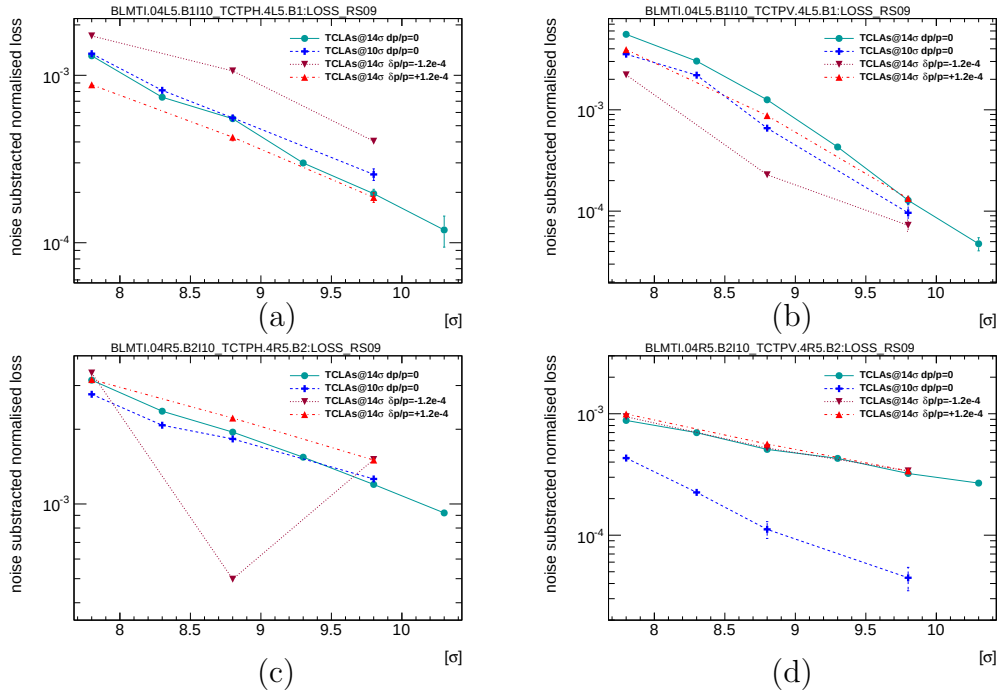


Figure 9: Losses on IR5 TCTs for B1 (a,b) and B2 (c,d) for scan 1 to 4.

# 4 First comparison to simulations

The TCT losses in scan 1 described in Sec. 3.2 are compared to SixTrack simulations of the cleaning around the ring, using a setup similar to Ref. [7]. Fig. 10 shows the measured and simulated losses versus TCT setting. It should be noted that the simulated values are the ratio of the number of protons lost in each TCT to the number of protons lost on the TCP. For the measurements, we show instead the ratio of the BLM signals at the TCTs and the highest signal in the ring, just downstream of the TCP. Since the material and length of these collimators are different, the BLM signal per lost proton is known not to be the same.

A qualitative agreement can be observed in Fig. 10, where the general trend of increasing losses with smaller TCT settings is well reproduced, as well as the approximate slope of the increase, which is similar for most TCTs. However, the measured losses are overall significantly higher than the simulated ones. This is expected because of the different materials and geometries at the TCT and the TCP, which influence the propagation of the hadronic and electromagnetic showers and therefore make the BLM signal per lost proton much higher at the TCTs [7]. Therefore, the measured ratio of BLM signals overestimates the fraction of protons lost on the TCTs.

This is seen quantitatively in Fig. 11, which shows the ratio between measurements and simulations. It should be noted that most measured signals are up to a factor 10 higher than in the measurements. This order of magnitude is compatible with the difference in BLM response calculated with FLUKA for other studies [8, 9, 10], although this particular case would have to be simulated in detail for a full comparison. A clear exception to this is the TCTPH.4R1.B2, which shows up to a factor 80 higher loss fraction in the measurements. This is not well understood. Such a large discrepancy due to the BLM response is unlikely. A possible explanation could be imperfections of the machine, e.g. an angular misalignment of the collimator tank, which could make the effective setting in $\sigma$ smaller than the one applied, or imperfections in the orbit or optics.

It should be noted in Fig. 10 that the simulations predict a larger slope of TCTPV.4L5.B1 than for the other TCTs. It has among the smallest loss fractions at large TCT settings, while it has the highest fraction at small settings. The SixTrack simulations show that losses on this collimator are dominated by particles coming directly from the vertical TCP, where they have undergone nuclear elastic scattering. This trend is very well reproduced by the measurements and can be understood from the normalized linear vertical phase space $(Y, P)$ illustrated in Fig. 12. It shows the cuts of the vertical collimators in IR7, as well as the vertical TCTs in IR1 and IR5. The TCP has been placed at phase zero. With this phase convention, and if we assume that the diffusion is slow enough that particles hit the TCP when they are at their maximum spacial amplitude in the betatron motion, any halo particle hitting the TCP would do so close to $P = 0$ and with a large enough $Y$-component to reach the cuts of its jaws (vertical lines).

A particle that undergoes nuclear elastic scattering in the TCP receives an angular kick so that it acquires an amplitude also along the $P$-axis. If it is scattered out of the TCP, it is clear from Fig. 12 that it can then directly impact the TCTPV.4L5.B1 (yellow cuts), without being intercepted by any secondary collimator in between. The closer this TCT is moved to the beam, the smaller scattering angle is needed to hit it, which means that the losses increase abruptly at smaller settings. On the other hand, the phase space areas covered by

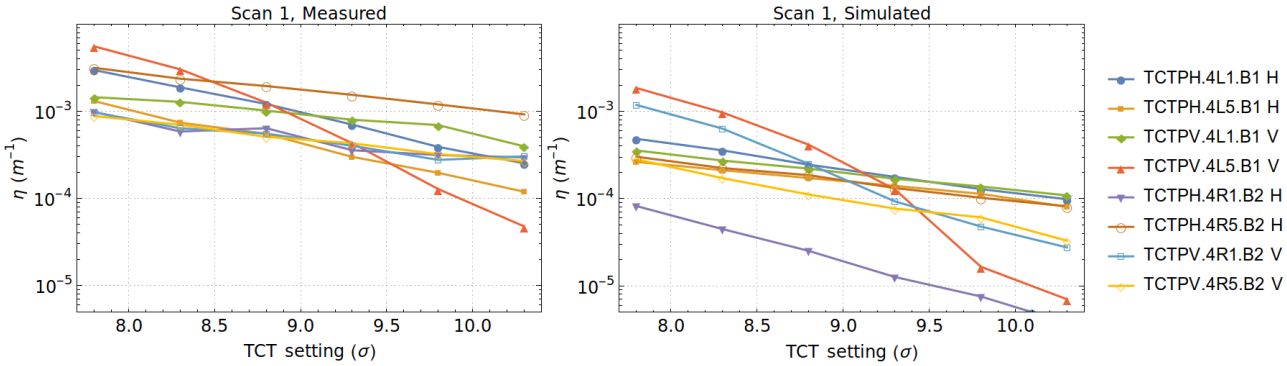


Figure 10: The measured and simulated losses from scan 1 (see Table 1) on the TCTs in IR1 and IR5, normalized by the loss at the TCP, as a function of the TCT setting. We show for each TCT the losses produced by the halo in the same plane.

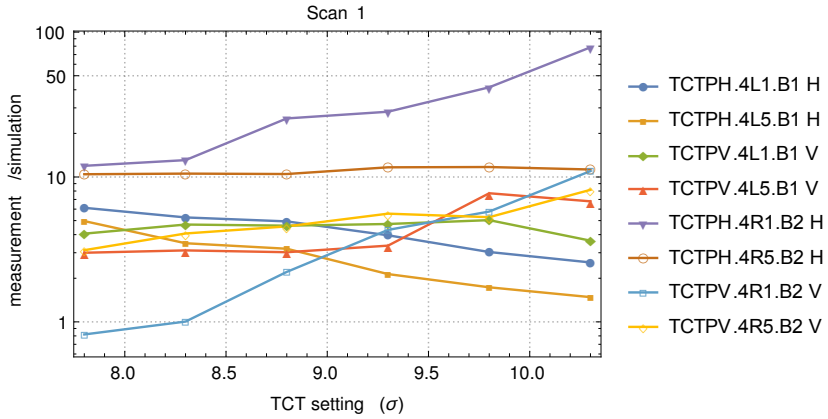


Figure 11: The ratio of measured and simulated losses from scan 1 (see Table 1) on the TCTs in IR1 and IR5, normalized by the loss at the TCP, as a function of the TCT setting. We show for each TCT the losses produced by the halo in the same plane.

TCTPV.4L1.B1 which are next to the TCP cuts are shielded by the TCSG.D4L7.B1, which means that this TCT receives significantly fewer impacts and that these are dominated by tertiary halo.

Simulations predict a similar behavior for TCTPV.4R1.B2, however, this is less visible in measurements. This is not understood in detail but possible explanations could involve machine imperfections. It is also possible that, at larger TCT settings, the BLM signal at this TCT is influenced by BLM cross-talk from the losses on the upstream horizontal TCT, which could change the slope. Since the horizontal TCTs are just upstream of the vertical ones, the BLM of the vertical TCT are impacted by shower particles not only from the vertical TCT but also from the horizontal one. The cross-talk in the opposite direction exists also, due to back-scattering of particles, but is less pronounced [7]. Therefore, for a complete comparison, the simulated losses on the neighboring TCTs would have to be weighted by appropriate factors.

Similar conclusions hold for the comparison of scan 2, for which the ratio of measured and simulated TCT ratios is shown in Fig. 13. In most cases the ratios are close to the

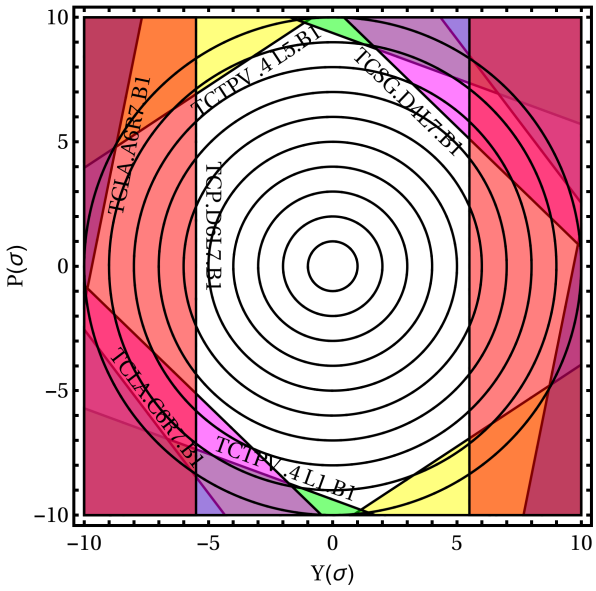


Figure 12: The normalized linear vertical phase space in the $\beta^*$=40 cm optics used in the MD. The symmetric cuts of the two jaws of vertical collimators are indicated and it is assumed that the vertical TCP is at a phase of zero in order to illustrate the situation for a particle scattered out of this collimator. It should be noted that the TCLAs have been positioned further in (9.5 $\sigma$) than in the MD to enhance visibility. The circles represent lines of constant phase space density at every $\sigma$.

corresponding results for scan 1 in Fig. 11. Furthermore, Fig. 14 shows the ratio of the TCT losses between scan 2 and scan 1 in measurements and simulations. This shows the effect of the closer TCLAs. In this comparison, we depend less on the BLM response, which cancels in the relative comparison if we assume it constant. The overall agreement is rather good, with many TCTs having only a moderate reduction in losses when the TCLAs are moved in from 14 $\sigma$ to 10 $\sigma$. The most significant improvement in losses with tight TCLAs is seen at TCTPV.4R5.B2 in both measurements and simulations. The underlying reason for this is still to be investigated.

The scans with energy offsets have not yet been studied in simulations.

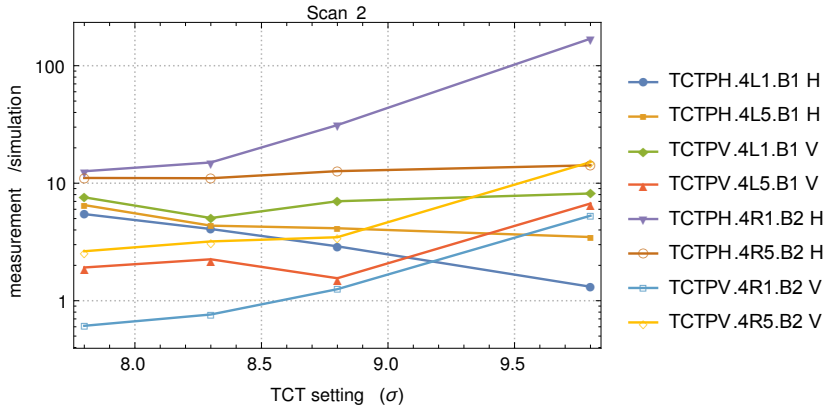


Figure 13: The ratio of measured and simulated losses from scan 2 (see Table 1) on the TCTs in IR1 and IR5, normalized by the loss at the TCP, as a function of the TCT setting. We show for each TCT the losses produced by the halo in the same plane.

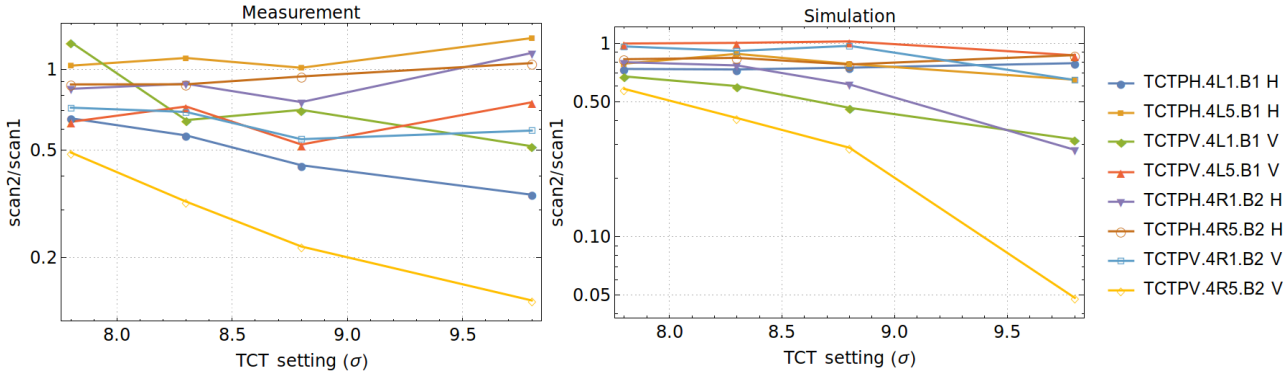


Figure 14: The ratio of normalized TCT losses between scan 2 (TCLAs at 10 $\sigma$) and scan 1 (TCLAs at 14 $\sigma$) in measurements and simulations, as a function of the TCT setting. We show for each TCT the losses produced by the halo in the same plane.

# 5 Asynchronous beam dump

After the loss maps, at the end of the MD, an asynchronous dump test was performed in order to study the losses on the TCTs in a tight configuration. The deployed collimator settings are shown in Table 1. The TCTs were moved to a setting of 7.8 $\sigma$, which is 1 $\sigma$ inside the 8.8 $\sigma$ setting tentatively proposed earlier [2]. The standard orbit bump was introduced in IR6, which brings the beam 1.2 mm further away from the TCDQ. This corresponds to a loss of 2.4 $\sigma$ margin in IR6, which is larger than expected from optics correction and studies of orbit variations [11, 12].

Putting together the effective loss of margin at the TCTs and in IR6, a total of 3.4 $\sigma$ is obtained. It should be noted that this is an extremely pessimistic case. Previous analysis of the margins, dominated by orbit and optics imperfections, based on Run I data, show that about 2 $\sigma$ are needed between TCTs and TCDQ [13] for the TCT to be shadowed by the TCDQ during 99% of the time spent in stable beams, as required with the philosophy adapted in Ref. [1]. In the configuration at $\beta^*$=40 cm, where we would rely on the phase

advance between dump kickers and the TCTs to reduce the margins, the direct shadowing no longer applies. However, we can still evaluate the probability for a certain loss of margin with an equivalent procedure, which in this case corresponds to the TCT going in to a setting where it risks to be damaged. Therefore, it is clear the implemented scenario is much more pessimistic than what can be expected during standard machine operation.

To perform the asynchronous dump test, the RF was turned off to make the beam debunch and drift longitudinally and the BSRA was used to monitor the abort gap population. The bunches closest to the abort gap drifted in there first (bucket 1 in B1 and bucket 401 in B2 as shown in Fig. 1). Since the bunch in B1 was much closer, the abort gap in B1 had a significantly higher population. Fig. 15 shows the measured bunch profiles in the abort gap at different times in B1 and B2. At the moment of the dump, the integrated abort gap population was $3.2 \times 10^{10}$ protons in B1 and $8.8 \times 10^{9}$ protons in B2.

It can be seen in Fig. 15 how the bunches enter the abort gap from the right (bucket 1) and move to the left at the same time as they spreads out. It should be noted that, due to this non-homogeneous population in the abort gap, the results of the asynchronous dump test cannot be scaled directly by the abort gap intensity to estimate losses during an asynchronous dump in physics. Instead, the losses at a certain element, such as a TCT, would have to be weighted by the relative abort gap population over the time interval where the losses are generated.

A dump was triggered when a maximum abort gap population was estimated online by monitoring the BSRA. The abort gap distributions at the time of the dump is shown in Fig. 16. In this figure, the horizontal axis has been scaled by the expected normalized kick in $\sigma$ as a function of time in the abort gap, assuming the ideal MKD kicker waveform and that all kickers fire simultaneously. The gray band indicates the range 6–12 $\sigma$ that could potentially cause impacts on the TCTs. As can be seen, it is only a small fraction of the abort gap. Figs. 15 and 16 show that if we had waited longer, the bunches would have drifted more to the left and we would have had a higher population in the gray band and thus better resolution of the losses on the TCTs. Nevertheless, all recorded TCT losses during the dump were well above the noise level.

The resulting loss distribution at the time of the dump is shown in Fig. 17, using the 40 $\mu$s integration time and normalized to the highest signal. As can be seen, the main loss location is in IR6 as expected, although these BLMs show a clear saturation. Significant losses leak to IR7, and also the TCTs in IR1 and IR5 are well visible. The losses on these TCTs were studied in detail and the results are shown in Fig. 18, together with simulation results.

In order to have a meaningful comparison with the simulations, we convert the measured TCT BLM signals to the estimated number of protons impacting the TCT. For this, the conversion factor of Gy/p is needed. It depends on the local geometry and the materials that the induced showers have to pass to reach the BLM. For our purposes, we extract an estimate from the previous MD on aperture measurements at $\beta^*$=40 cm in Ref. [14]. During a part of this MD, the TCTs were the primary bottleneck of the ring while losses were excited. We can then divide the BLM signal by the measured intensity decay. The obtained factor is, averaged over five measurements, $2.1 \times 10^{-11}$ Gy/p. This is a factor 3–4 lower than what was calculated for halo cleaning losses with FLUKA [10] at 7 TeV. It should be noted, however, that for these numbers, the impact distribution on the TCTs was not the same, and likely

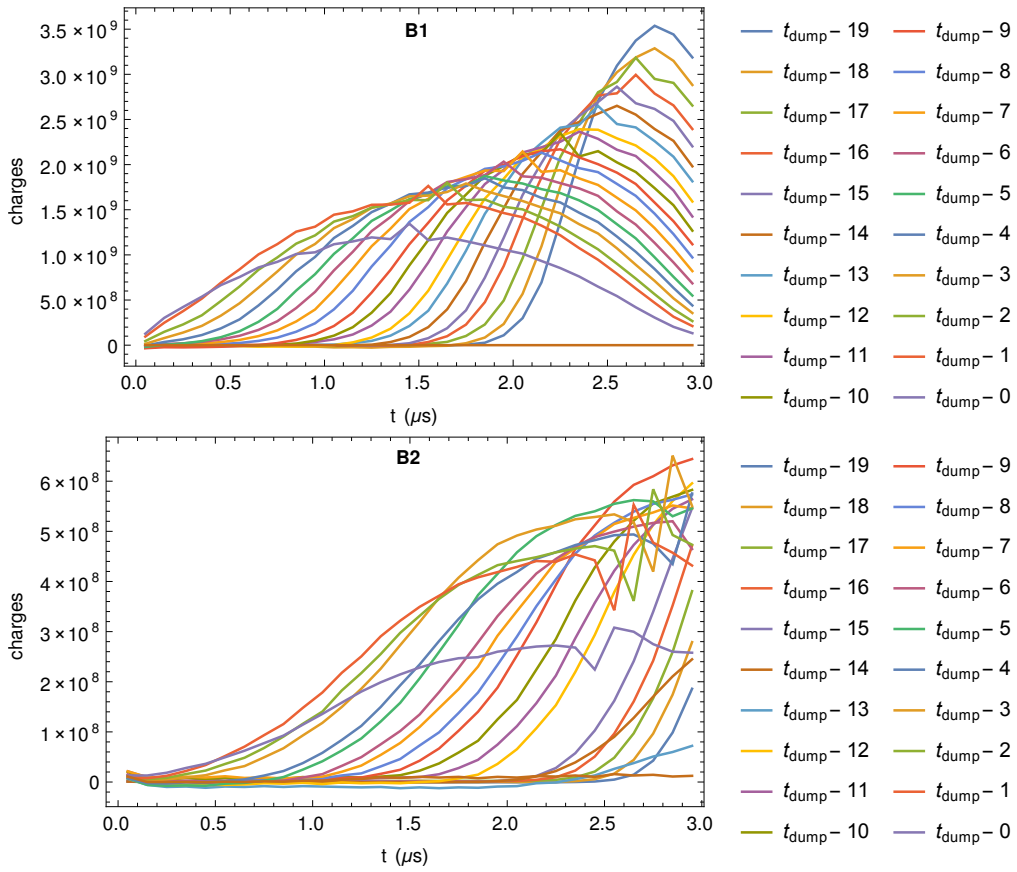


Figure 15: The longitudinal beam profiles along the abort gap, as measured by the BSRA, during the 20 s preceding the asynchronous dump test. It can be seen that the population in B2 (bottom) is significantly lower than in B1 (top).

not corresponding to the one during the asynchronous beam dump test, which introduces an uncertainty. In order to stay conservative, i.e. rather overestimate than underestimate the number of protons on the TCT, we use the lower conversion factor $2.1 \times 10^{-11}$ Gy/p from the aperture measurements.

The simulations of an asynchronous beam dump have been carried out with SixTrack, using the setup described in Ref. [1]. It was assumed that all dump kickers fire simultaneously, as in the measurement. A train of 25 ns bunches with equal bunch populations was simulated, while in the measurements the abort gap was not homogeneous as shown in Fig. 16. Therefore, each bunch in the simulation was normalized to the measured population over the corresponding 25 ns interval, and in the end the losses at the TCTs were summed over all bunches.

As can be seen, the final comparison in Fig. 18 between measurements and simulations show, except at TCTPH.4R1.B2, an agreement within a factor 3. We consider this a good agreement, which is in line with the uncertainties found in previous comparison between measured and simulated BLM signals [7]. Several uncertainties can be identified, which could explain the discrepancy, e.g. that the BLM response factor could be different in this particular loss scenario than in the aperture measurements, and that the BLM response might

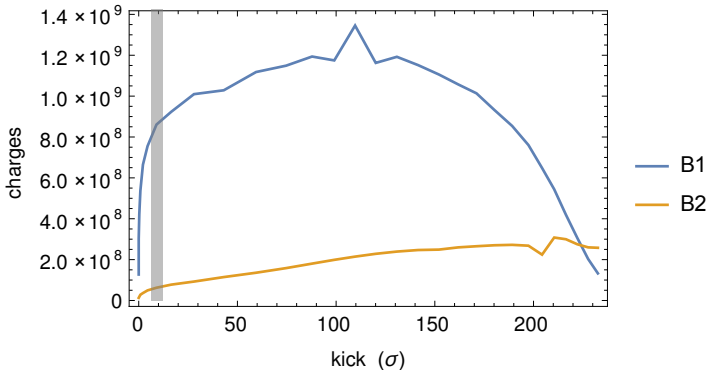


Figure 16: The longitudinal beam profiles for both beams along the abort gap, as measured by the BSRA, at the time when the dump was triggered. The abort gap population is given as a function of total kick in $\sigma$, summed over all MKDs, and assuming that all kickers fire at the same time with the ideal waveform. The gray band indicates the region where particles could end up at the TCTs.

be different depending on the exact BLM placement and impact distribution. Furthermore, the exact beam distribution in the measurement was not known in detail (a Gaussian was assumed in the simulations) and random machine imperfections were not included.

Based on the comparison, we conclude that the simulations work well within the expected accuracy for three TCTs, however, at TCTPH.4R1.B2 a discrepancy of about factor 20 is found. This is significantly larger than what can be reasonably expected within the given uncertainties. This is not fully understood, but it should be noted that the same TCT gave a much higher BLM signal than expected also in the loss maps (see Sec. 4). A possible explanation could be that, for this TCT, the BLM response would be very different from the other TCTs, e.g. due to the BLM placement or the electronics. It could also be that this TCT was effectively closer to the beam than thought, e.g. due to a misalignment of the collimator tank in the tunnel or orbit and optics imperfections.

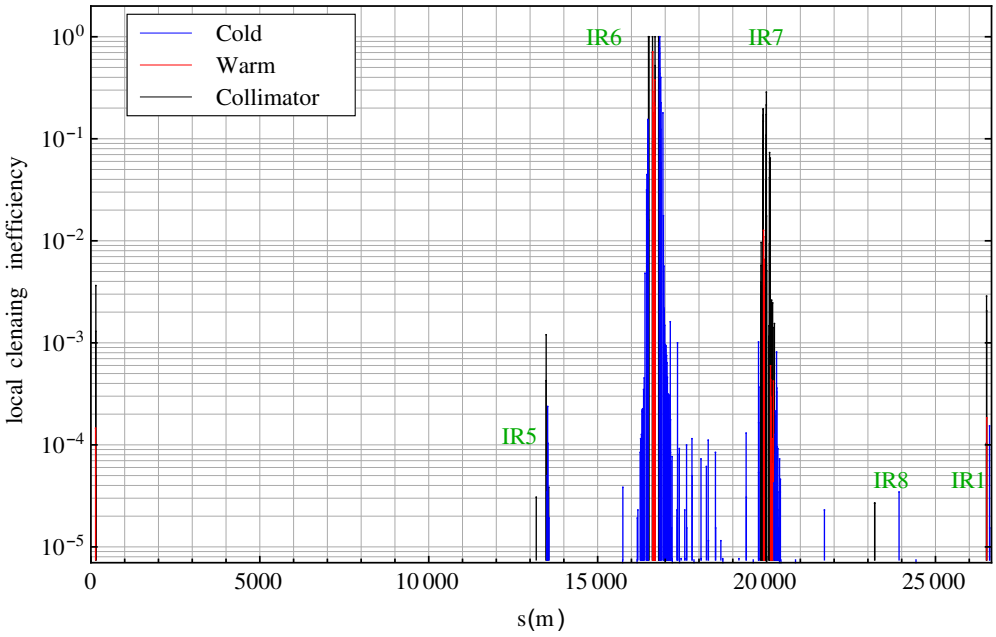


Figure 17: The measured loss map distribution around the ring at the time of the asynchronous dump test, using a 40 $\mu$s integration time on the BLMs. All signals have been normalized to the highest one.

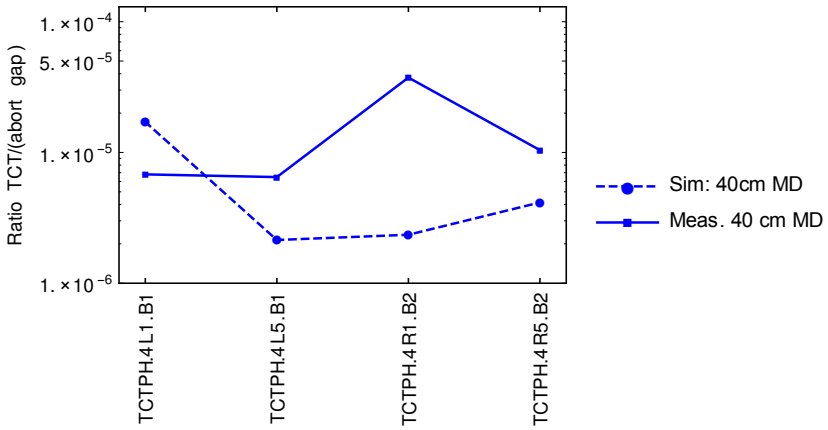


Figure 18: The ratio of the total abort gap population hitting the TCTs in IR1 and IR5 during the asynchronous dump test, as estimated from the BLM signals and converted to protons, using the conversion factor from Ref. [14]. The measurements are compared to SixTrack simulations that have been normalized by the measured abort gap profile in Fig. 16.

# 6 Conclusions

We have presented the results of MD 310, in which a total of 70 betatron loss maps were performed. The results show that no issues in terms of cleaning are expected with the nominal $\beta^*$=40 cm optics with the proposed 2 $\sigma$ retraction collimator settings. Furthermore, the measurements confirm an increase of losses on the TCTs in IR1 and IR5 at tight settings, which was predicted by SixTrack simulations. Compared to the loss maps with standard $\beta^*$=80 cm optics [4], about a factor 10 more losses is observed with the TCTs at 8.8 $\sigma$. A part of this increase could possibly be recovered by closer TCLA settings, although the risk of impacts on the TCLAs during an asynchronous beam dump would have to be studied in detail. The higher TCT losses are expected to cause the experimental background to increase by the same factor. ATLAS and CMS were taking data during the MD to monitor this. The analysis of this is ongoing in ATLAS and CMS in order to conclude on if it is acceptable for operation.

The MD was finished with an asynchronous beam dump test, where the TCTs in IR1 and IR5 were moved to a very tight setting of 7.8 $\sigma$, which is 1 $\sigma$ further in than the proposed setting. Furthermore, we used an orbit bump in IR6 that moves the beam away from the TCDQ by 2.4 $\sigma$. The used configuration, with a total loss of 3.4 $\sigma$ margin between TCDQ and TCT, is therefore a lot more pessimistic in terms of lost margin than can be expected in the real machine, where we do not expect this to exceed about 2 $\sigma$. The measured losses during the dump are reproduced by simulations within a factor 3, which we consider a good agreement in view of various uncertainties, except at TCTPH.4R1.B2, where a factor 20 discrepancy is found. The same collimator showed also much higher losses than expected from simulations in the betatron loss maps. It is not well understood whether this is an artifact of the BLM (placement or electronics) or if it is caused by this collimator being closer to the beam than expected due to e.g. a tank misalignment. Further studies should be made to conclude on whether the asynchronous beam dump can still be considered safe in the proposed configuration.

This MD is part of a series of MDs intended to explore the LHC $\beta^*$-reach in Run II. Combining the results of all MDs, we hope to conclude on the the feasibility of $\beta^*$=40 cm or below.

# 7 Acknowledgments

We would like to thank the OP crew for their assistance during the MD and in particular M. Solfaroli for the preparation of the filling scheme. Furthermore, we are grateful to C. Bracco, M. Fraser and J. Uythoven for discussions of the asynchronous beam dump data.

# References

[1] R. Bruce, R. W. Assmann, and S. Redaelli. Calculations of safe collimator settings and $\beta^*$ at the CERN Large Hadron Collider. *Phys. Rev. ST Accel. Beams*, 18:061001, Jun 2015.

[2] R. Bruce. Update on possibilities to reach $\beta^*$=40cm. *presentation in the LHC Collimation Working Group, 2015.01.19*, 2015.

[3] A. Langner, F. Carlier, J. Coello de Portugal, A. Garcia-Tabares Valdivieso, E.H. Maclean, L. Malina, T.H.B. Persson, S. Mönig, B. Salvachua Ferrando, P. Skowronski, R. Tomas, and J. Wenninger. LHC optics commissioning with $\beta^* = 40$ cm and 60 cm. *CERN-MD-Note-2015-?*, 2015.

[4] D. Mirarchi. Status of loss map validation. *presentation in the LHC Collimation Working Group, 2015.06.22*, 2015.

[5] A. Mereghetti, R. Bruce, R. Kwee, D. Mirarchi, E. Quaranta, S.Redaelli, A. Rossi, R. Rossi, B. Salvachua Ferrando, and A. Valloni. IR7 collimation hierarchy and impedance. *CERN-MD-Note-2015-?*, 2015.

[6] R. Bruce, R.W. Assmann, V. Boccone, G. Bregliozzi, H. Burkhardt, F. Cerutti, A. Ferrari, M. Huhtinen, A. Lechner, Y. Levinsen, A. Mereghetti, N.V. Mokhov, I.S. Tropin, and V. Vlachoudis. Sources of machine-induced background in the ATLAS and CMS detectors at the CERN Large Hadron Collider. *Nucl. Instrum. Methods Phys. Res., Sect. A*, 729(0):825 – 840, 2013.

[7] R. Bruce, R. W. Assmann, V. Boccone, C. Bracco, M. Brugger, M. Cauchi, F. Cerutti, D. Deboy, A. Ferrari, L. Lari, A. Marsili, A. Mereghetti, D. Mirarchi, E. Quaranta, S. Redaelli, G. Robert-Demolaize, A. Rossi, B. Salvachua, E. Skordis, C. Tambasco, G. Valentino, T. Weiler, V. Vlachoudis, and D. Wollmann. Simulations and measurements of beam loss patterns at the CERN Large Hadron Collider. *Phys. Rev. ST Accel. Beams*, 17:081004, Aug 2014.

[8] R. Bruce and E. Skordis. Predictive power of SixTrack+FLUKA: Comparison between simulated and measured loss maps. *presentation in the LHC Collimation Working Group, 2013.05.06*, 2013.

[9] E. Skordis *et al.* Updates on FLUKA simulations of the 4 TeV quench test. *presentation in the LHC Collimation Working Group, 2014.10.06*, 2014.

[10] F. Cerutti. Collimator load and BLM response. *presentation in the LHC Collimation Working Group, 2014.08.25*, 2014.

[11] R. Bruce. Status of collimation analysis for $\beta^*$=40cm. *presentation in the LHC Collimation Working Group, 2015.10.05*, 2015.

[12] G. Valentino and A. Valloni. Analysis of collimator BPMs during the machine cycle. *presentation in the LHC Collimation Working Group, 2015.10.05*, 2015.

[13] R. Bruce and S. Redaelli. Collimation and $\beta^*$-reach. *Proceedings of the 5th Evian Workshop, Evian, France*, 2014.

[14] R. Bruce, P. D. Hermes, H. Garcia, R. Kwee-Hinzmann, A. Mereghetti, D. Mirarchi, S. Redaelli, P. Skowronski, G. Valentino, and A. Valloni. IR aperture measurement at $\beta^*$=40 cm. *CERN-ACC-NOTE-2015-0037*, 2015.